ISSN 2075-1133, Inorganic Materials: Applied Research, 2022, Vol. 13, No. 2, pp. 277–293. © Pleiades Publishing, Ltd., 2022.
Russian Text © The Author(s), 2021, published in Perspektivnye Materialy, 2021, No. 9, pp. 5–23.

PHYSICOCHEMICAL FUNDAMENTALS OF CREATING MATERIALS AND TECHNOLOGIES

Prediction of Space Groups for Perovskite-Like $A_2^{II}B^{III}B'^{V}O_6$ Compounds

N. N. Kiselyova[a, *], V. A. Dudarev[a, b, **], A. V. Stolyarenko[a, *], A. A. Dokukin[a, c, ****], O. V. Sen'ko[c, *****], V. V. Ryazanov[c, ******], M. A. Vitushko[d, *******], V. S. Pereverzev-Orlov[d, ********], and E. A. Vaschenko[d, *********]**

[a] *Baikov Institute of Metallurgy and Materials Science, Russian Academy of Sciences, Moscow, 119334 Russia*
[b] *Higher School of Economics, National Research University, Moscow, 101000 Russia*
[c] *Federal Research Center Computer Science and Control, Russian Academy of Sciences, Moscow, 119333 Russia*
[d] *Kharkevich Institute for Information Transmission Problems, Russian Academy of Sciences, Moscow, 127051, Russia*

**e-mail: kis@imet.ac.ru*
***e-mail: vic@imet.ac.ru*
****e-mail: stol-drew@yandex.ru*
*****e-mail: dalex@ccas.ru*
******e-mail: senkoov@mail.ru*
*******e-mail: rvvccas@mail.ru*
********e-mail: vit@iitp.ru*
*********e-mail: slavaperor@gmail.com*
**********e-mail: vea@iitp.ru*

Received February 3, 2021; revised April 19, 2021; accepted April 20, 2021

Abstract—The prediction of new compounds having such composition as $A_2^{II}B^{III}B'^{V}O_6$ was carried out, the type of distortion of their perovskite-like lattice and the space group were predicted, and the crystal lattice parameters of the predicted compounds were estimated. For the prediction, only the property values of the chemical elements were used. The programs based on machine learning algorithms for different variants of neural networks, a linear machine, the formation of logical regularities, *k*-nearest neighbors, and support vector machine showed the best results when predicting the type of distortion of a perovskite-like lattice. When evaluating the lattice parameters, programs based on algorithms for orthogonal matching pursuit and automatic relevance determination regression were the most accurate methods. The prediction accuracy for the type of distortion of perovskite-like lattice was no less than 74%. The accuracy of estimating the lattice linear parameters was within ±0.0120–0.8264 Å, and the accuracy of angles β for the monoclinic distortion of the lattice amounted to ±0.08°–0.74°. The calculations were carried out using systems based on machine learning methods. To evaluate the prediction accuracy, an examination recognition in the cross-validation mode was used for the compounds included in the sample for machine learning. The predicted compounds are promising for searching for novel magnetic, thermoelectric, and dielectric materials.

Keywords: perovskite, crystal lattice parameter, predicting, machine learning
DOI: 10.1134/S2075113322020228

INTRODUCTION

Perovskite-like compounds are among the most studied inorganic substances. This is due to their different physical and chemical properties: magnetic [1–4], thermoelectric [4–6], dielectric [7, 8], catalytic [8, 9], etc. They can also be used as electrode materials for fuel cells [10, 11]. Some perovskites simultaneously combine different properties [12, 13], which expands the scope of their application.

The crystal structure of double perovskites, the compounds that have composition $A_2BB'O_6$, in many cases differs from the ideal cubic structure inherent in perovskite. The problem of predicting the crystal structure of double perovskites is to a significant extent connected with determining the type of distortions of the structure under preset external conditions. Most of the criteria developed to solve this problem take into account the size of ions. Let us consider the most popular of these criteria.

The classical criterion for determining the type of perovskite structure distortion is represented by tolerance factor *t*. In the case of double perovskites

$A_2BB'O_6$, this parameter can be written in the following form [14]:

$$t = \frac{r_A + r_O}{\frac{\sqrt{2}(r_B + r_{B'})}{2} + r_O},$$

where r_A is the ionic radius for coordination number 12, and r_B, $r_{B'}$, and r_O are the ionic radii for coordination number 6. According to this criterion, for an ideal cubic structure, t is close to 1. At $t < 0.77$, other structures are formed (such as ilmenite, corundum, etc.). If $0.77 < t < 1$, rhombic, tetragonal, monoclinic, or rhombohedral distortions are can occur. At $t > 1$, a hexagonal distortion of the ideal perovskite structure is observed.

All of the mentioned values of the tolerance factor are very approximate and different publications indicate different ranges for different types of distortions that often overlap. Thus, the tolerance factor can hardly be considered as a reliable rule for predicting possible distortions for the crystal lattice of double perovskites.

It should be noted that the most common reasons for a decrease in symmetry can be represented by rotation (tilt) of the chains of BO_6 and $B'O_6$ octahedra or by the distortion of these octahedra, as well as by the displacement of cations from ideal positions. At the same time, in most cases, the decrease in symmetry is associated with a combination of several reasons. Rotation and tilt of the octahedron chains are responsible for the most common type of distortion in double perovskites.

It was shown in [15] that 23 different systems of octahedron tilt are possible in the perovskite structure. Later, the authors of [16] on the basis of group-theoretical analysis showed that only 15 such tilt systems are nonequivalent, and possible space groups were derived depending on a particular tilt system of the octahedral framework. On the basis of the above-mentioned publications [15, 16], the authors of [17] developed a SPuDS (Structure Prediction Diagnostic Software) software system [17] designed to predict the type of perovskite structure distortion and to estimate the parameters of the crystal structure of ABX_3 perovskites.

For the calculations, a value of the cation-anionic interaction was used, in turn, the equation for the calculation of which includes the cation-anion distance, as well as an empirically chosen constant and a variable. It should be noted that the need to select the latter two components of the equation significantly reduces the efficiency of the proposed method. Then, using the obtained value of the cation-anionic interaction, a global instability index of was calculated. The latter was minimized by changing the tilt of octahedra (and the position of the A cation).

Then, the authors searched for the crystal structure that corresponds to the minimum value of this semiempirical instability index. If the calculated index did not exceed 0.1, then the structure was considered stable. Above 0.2, the structure was referred to as unstable. The lattice parameters could be calculated on the basis of the B–O distance and the tilt angle of the octahedra. The authors of [18] used the SPuDS system for compounds having such composition as $A_2BB'O_6$.

It should be noted that the tilt and distortion of octahedra, as well as the displacement of cations from the ideal positions of the cubic perovskite, do not cover all the reasons for the distortion of the ideal cubic perovskite structure. Other factors are possible, too, for example, Jahn–Teller effect, changing valence, the presence of vacancies, etc.

It is clear that neither the tolerance factor nor the method underlying SPuDS can completely take into account all these factors. Therefore, in recent years, researchers have paid attention to the methods of machine learning, which makes it possible to find complex regularities linking the properties of perovskites with the parameters of chemical elements that compose the compound on the basis of the analysis of information concerning already known $A_2BB'O_6$ compounds [19–25].

Namely machine learning methods have made it possible not only to predict new double perovskites but also to estimate some of their properties, for example, formation energy [19] and thermodynamic stability [21], crystal lattice parameters [20, 22], band gap [23], and octahedral tilt [24]. The distinctive feature of the approach to predicting novel inorganic compounds based on machine learning methods consists in including a wide set of the properties of chemical elements in the sought dependencies, rather than only dimensional parameters and data on the charge distribution.

In most applications of machine learning methods, this provides an increase in the accuracy of predictions. Since the number of known double perovskites is quite large, a significant confinement such as the representativeness of the sample for machine learning is removed when using these methods. It should be noted that, when predicting new inorganic compounds, only the properties of chemical elements are used.

CALCULATION METHODS

The first predictions for not yet synthesized ABO_3 perovskites were obtained in our investigations using machine learning methods in the middle of the 1970s [26]. The comparison of our results with new experimental data has shown that the prediction accuracy of the formation of compounds having this composition amounted to 90%, whereas for the structure of

cubic perovskite the prediction accuracy amounted to 85% [27].

This work is aimed at improving the prediction accuracy for the crystal structure type of $A_2^{II}B^{III}B'^{V}O_6$ compounds owing to using the ensembles of machine learning algorithms [28].

The fact is that earlier only one of these methods was used in predicting; for example, in [19, 21], there were different variants for training a random forest. Even in those publications, whose authors used different algorithms [24, 25], the final decision according to the results of prediction was made on the basis of a simple vote for most of the predictions using different methods.

In this work, we used collective decision-making methods for the predicting results based on special heuristics [28], the programs of which are included in our developed information-analytical system (IAS) for designing inorganic compounds [29]. At first, different machine learning algorithms included in the IAS were independently applied. Then, an optimal collective solution was automatically found using special corrector methods [28].

The development of such an approach was dictated by the impossibility of predicting in advance which machine learning algorithm would be most efficient in solving a specific chemical problem. The use of the ensembles of algorithms makes it possible to compensate for possible disadvantages of using one algorithm by using the advantages of other ones. As our long-term experience shows, the ensembles of machine learning algorithms in most cases provide an increase the predicting accuracy when solving chemical problems [30, 31].

The machine learning and predicting procedure includes several stages.

1. At the first stage, a selection of the examples of known compounds for machine learning is performed. The source of information is represented by the integrated database system (DB) of the Baikov Institute of Metallurgy and Materials Science concerning the properties of more than 85 000 inorganic compounds (http://www.imet-db.ru/), including information on more than 750 compounds having $A_2^{II}B^{III}B'^{V}O_6$ composition.

The selection of examples is the most difficult, time-consuming, and nonformalized task, the solution of which determines to a significant extent the accuracy of obtained predictions. In the present study, the complexity of the training sample formation was associated with extremely contradictory information on the type of distortion of an ideal perovskite crystal structure under normal conditions for most compounds.

For example, for compound Sr_2YSbO_6, different systems are indicated at a room temperature: monoclinic (space group $P2_1/n$ [32]) and orthorhombic [33]. According to different researchers, double perovskite Ba_2SmNbO_6 exhibits a tetragonal distortion type [34] (space group $I4/m$ [35]) and a monoclinic distortion type (space groups $P2_1/n$ [36] or $I2/m$ [37]).

One of the ways to resolve the ambiguities and to reduce the amount of analyzed information consists in the use special systems we have developed for determining anomalous objects, which are based on the idea of compactness of the classes of inorganic substances in the multidimensional space of the parameters of chemical elements [38, 39], which is a consequence of the periodic law.

In other words, substances that include a set of elements close in the values of parameters should be close to each other in crystal structure too. These software systems significantly reduce the time of the analysis of experimental information by means of pointing out to the expert those substances whose published type of crystal structure distortion does not fall into its own class.

For example, one of the methods for determining substances whose set of component values differs from the sets of such values for substances with the same space group is reduced to determining the magnitude of the examination recognition error when adding information on the evaluated substance to the training set [38]. If the error increases by more than the specified value, then this object is considered anomalous. It is natural that the final decision concerning the crystal structure of the falling-out substance is made by an expert in the field of the subject.

2. The selection of the parameters of chemical elements for including them in the desired regularity that makes it possible to predict the type of crystal structure for compounds is of great importance. The primary selection is carried out on the basis of physicochemical concepts of the nature of the substances under study and using a database of the properties of elements (http://phases.imet-db.ru/elements).

In addition, a special program generates algebraic functions of the parameters of elements using a set of elementary algebraic operations on the values of parameters having the same type in physical meaning and dimension. Further, using the program [40] included in the IAS, the importance for the classification of the initial properties of the elements and for the classification of generated functions is estimated.

Using the visualization system, one can show any projection of points onto a plane the coordinates of which are any pair of chosen parameters of the elements or their functions, which facilitates the interpretation of the results.

The result of these two stages represents a matrix (training sample), each row of which corresponds to a set of values of the properties of the elements that form the experimentally investigated $A_2^{II}B^{III}B'^{V}O_6$ com-

Table 1. Results of importance evaluation for classifying the parameters of elements and choosing the most accurate machine learning methods

Task	The most important parameters of the elements	Prediction accuracy using properties of elements and the most important parameters, %	Prediction accuracy using only the properties of elements, %	Selected machine learning methods
Multiclass predicting	A2(B)/M11(A); A4(B')+M7(B); A3(B')/M7(B)	**74**	74	(linear machine, logical regularities formation, *k*-nearest neighbors, support vector machine)—majority vote
Prediction of compounds with space group $P6_3/mmc$	I8(A)/I8(B')	**100**	96	(estimates calculation algorithms, neural network training, *k*-nearest neighbors)—major-ity vote
Prediction of compounds with space group *Pbnm*	A4(B')/A3(A)	97	**99**	(linear machine, multilevel perceptron, neural network training, support vector machine)—convex stabilizer
Prediction of compounds with space group *I*2/*m*	I11(B)*I11(B'); I10(A)/I10(B)	**99**	99	(neural network training, *k*-nearest neighbors, support vector machine)—convex stabilizer
Prediction of compounds with space group *I*4/*m*	E8(A)/E8(B')	**97**	94	(linear machine, *k*-nearest neighbors, neural network training)—averaging
Prediction of compounds with space group *Fm*(−)3*m*	A2(B')+M7(B)	85	83	(linear machine, neural network training, *k*-nearest neighbors, support vector machine)—generalized polynomial corrector
Prediction of compounds with space group $P2_1/n$	A2(B')/M6(A); E7(A)-E7(B'); E6(B)*E7(B')	91	93	(linear machine, *k*-nearest neighbors, neural network training, support vector machine) - averaging
Prediction of compounds with space group *Pm*(−)3*m*	A2(A)/A4(B')	94	**98**	(neural network training, *k*-nearest neighbors, support vector machine)—clustering and selection
Prediction of compounds with space group *R*(−)3	A3(B')/M11(A)	94	**96**	(multilevel perceptron, *k*-nearest neighbors, neural network training, support vector machine)—the Woods dynamic method

Table 2. Results of accuracy evaluation for predicting the crystal lattice parameters of compounds $A_2^{II}B^{III}B'^{V}O_6$

Task	Space group (Sp.gr.), parameter	Algorithm	Determination coefficient R^2	Mean absolute error, MAE	Mean square error, MSE
1	*I*2/*m*, *a*	Elastic Net	0.95	0.0251	0.0018
2	*I*2/*m*, *b*	Orthogonal Matching Pursuit	0.96	0.0486	0.0364
3	*I*2/*m*, *c*	Linear Regression	1.00	0.0677	0.0235
4	*I*2/*m*, β	ARD Regression	0.99	0.7359	3.5439
5	*I*4/*m*, *a*	Ridge	1.00	0.0120	0.0005
6	*I*4/*m*, *c*	Random Forest	0.99	0.0163	0.0007
7	*Fm*(–)3*m*, *a*	ARD Regression	0.81	0.0725	0.0520
8	$P2_1/n$, *a*	ARD Regression	0.98	0.0181	0.0019
9	$P2_1/n$, *b*	Convex with loop reduction	0.93	0.0234	0.0013
10	$P2_1/n$, *c*	Ridge	0.66	0.0438	0.0434
11	$P2_1/n$, β	SAND	0.78	0.0794	0.0335
12	$P6_3/mmc$, *a*	ARD Regression	0.99	0.0201	0.0014
13	$P6_3/mmc$, *c*	ARD Regression	1.00	0.8264	3.5610
14	*Pbnm*, *a*	ARD Regression	0.99	0.1256	0.0562
15	*Pbnm*, *b*	Orthogonal Matching Pursuit	0.97	0.1758	0.1934
16	*Pbnm*, *c*	Orthogonal Matching Pursuit	0.97	0.3931	0.5264
17	*Pm*(–)3*m*, *a*	Orthogonal Matching Pursuit	0.93	0.0230	0.0076
18	*R*(–)3, *a*	SAND	1.00	0.7839	2.4921
19	*R*(–)3, *c*	ARD Regression	1.00	0.7411	1.6414

pound with the designation of a space group to which this compound belongs.

3. In order to predict novel double perovskites, we used two systems that we developed. The first information analytical system [29] was used to predict the type of distortion of a crystal structure (space group). The second system ParIS (Parameters of Inorganic Substances) [41] was used to estimate the crystal lattice parameters of double perovskites. The IAS data analysis subsystem currently includes 15 machine learning programs and nine programs for collective decision making [29, 30].

The data analysis subsystem of the ParIS system includes 11 machine learning programs [41]. In the course of machine learning, the most accurate algorithms were chosen, which were then used for searching for regularities and for predicting. To assess the accuracy (the ratio of the number of substances for which the assigned classes have been correctly recognized to the total number of recognized substances), in the IAS, we used such a widespread procedure as examination recognition with cross-validation on the material of the training sample. This procedure is described in detail by the authors of [30].

When making a collective decision in the IAS, the most accurate algorithm was also chosen too, for which we used the examination recognition of a set amount of substances randomly chosen from training samples and not used in machine learning (at the final stage of predicting, the reference cases were returned to the training sample).

The subsystem for assessing the quality of learning in the ParIS system makes it possible to estimate the mean absolute error (MAE) and mean squared error (MSE) with cross-validation in the Leave-One-Out Cross-Validation (LOOCV) mode, the coefficient of determination R^2, etc., as well as to construct a diagram of the deviations of the calculated values of the parameters from the experimental ones for the substances the information concerning which was used in machine learning.

4. The prediction was carried out by means of special IAS and ParIS subsystems using only the values of the properties of the elements composing the predicted substance. First of all, using the IAS, the prediction of belonging to the most common space groups was carried out at room temperature and at atmospheric pressure. This task was divided in two.

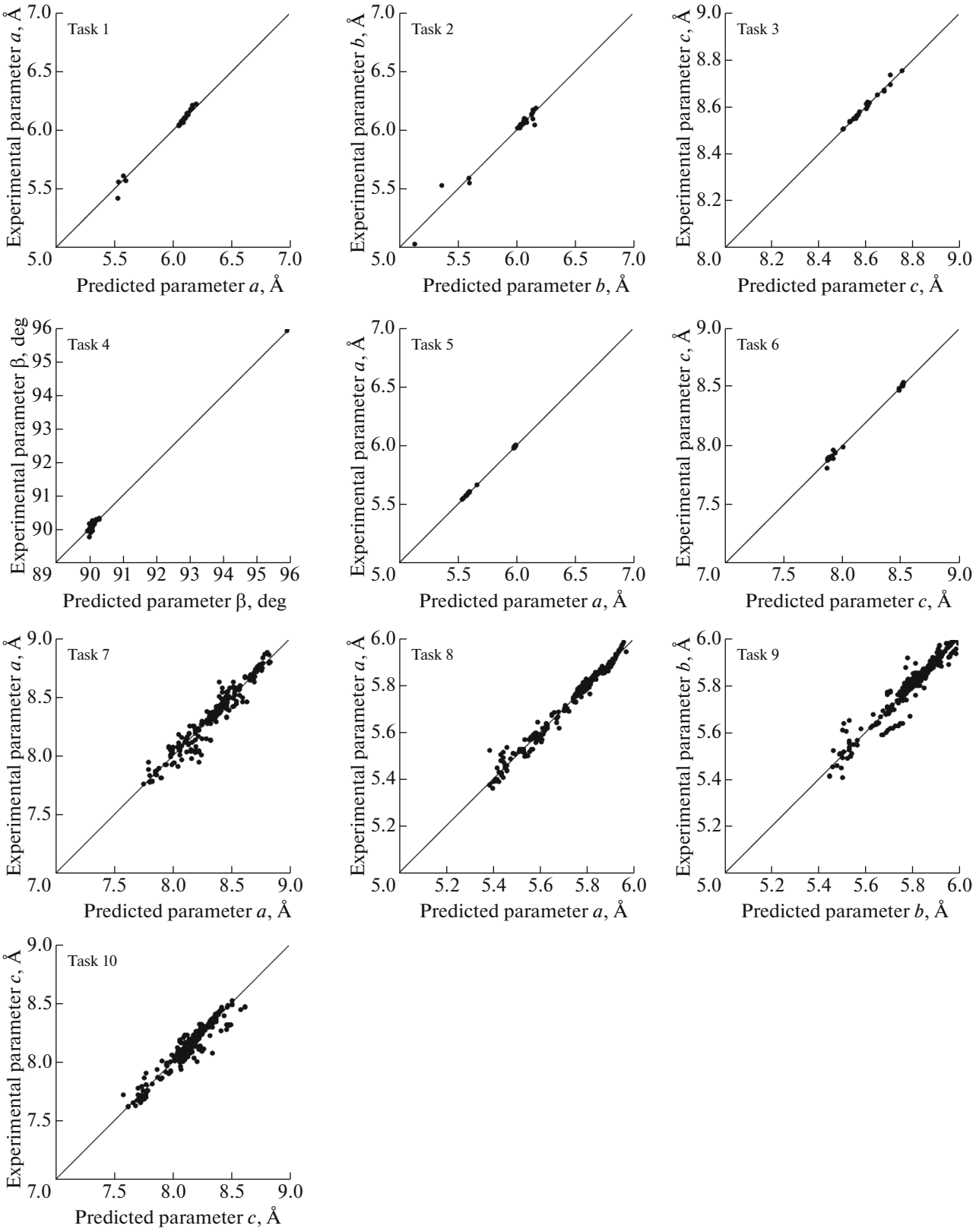

Fig. 1. Diagrams of deviations of the predicted lattice parameters from the experimental ones in tasks 1–10 (see the list of tasks in Table 2).

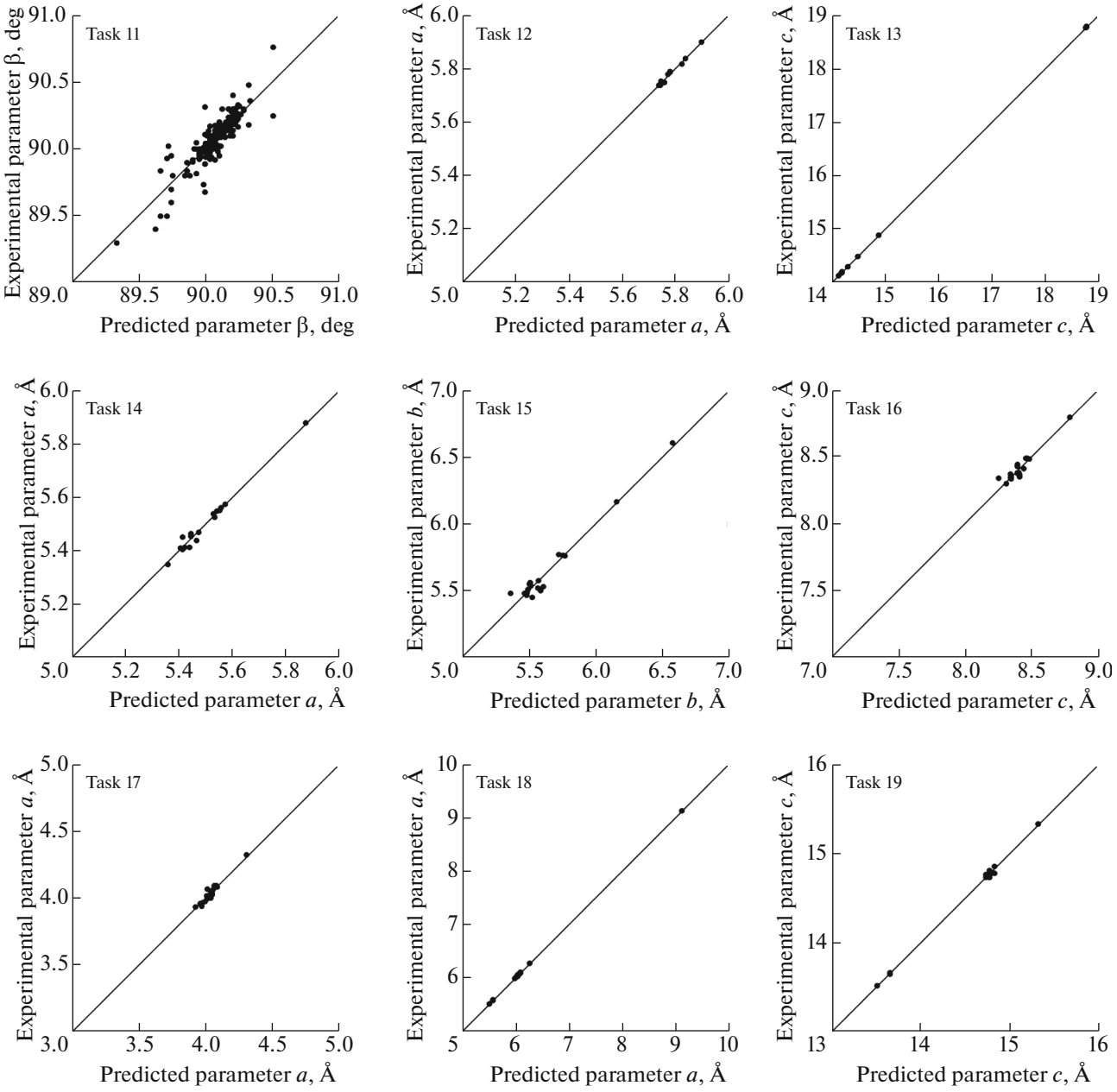

Fig. 2. Diagrams of deviations of the predicted lattice parameters from the experimental ones in tasks 11–19 (see the list of tasks in Table 2).

Initially, for the compounds having composition $A_2^{II}B^{III}B'^{V}O_6$, a multiclass prediction of belonging to nine of the classes was carried out: compounds with the structure of an ideal cubic perovskite (space group $Pm(-)3m$), compounds with space groups $P2_1/n$, $Fm(-)3m$, $I2/m$, $Pbnm$, $I4/m$, $R(-)3$, $P6_3/mmc$, and compounds with a structure different from the one given above; and then a sequential separation of $A_2^{II}B^{III}B'^{V}O_6$ compounds into two classes was performed, for example, target class 1—the phases with the structure of ideal cubic perovskite, and class 2—the compounds with a structure different from ideal cubic perovskite.

The final result of prediction was formed on the basis of comparing the predictions obtained when fulfilling all the tasks. If the results contradicted each other, then the prediction was considered uncertain. Then, using the ParIS system for the predicted com-

Table 3. Prediction of parameter *a* for the cubic crystal lattice of new $A_2^{II}B^{III}B'^{V}O_6$ compounds

Composition	*a*, Å	Composition	*a*, Å	Composition	*a*, Å
Sp. gr. *Fm*(−)3*m* (algorithm ARD Regression)					
Ca_2AlUO_6	7.9030	Sr_2PmUO_6	8.5299	Ba_2PmWO_6	8.5261
Ca_2ScUO_6	8.1164	Sr_2TbUO_6	8.5152	Ba_2PmMoO_6	8.4351
Ca_2GaUO_6	8.0806	Sr_2TmUO_6	8.4477	Ba_2PmUO_6	8.7044
Ca_2YUO_6	8.3583	Sr_2BiUO_6	8.6795	Ba_2GdRuO_6	8.3499
Ca_2PrUO_6	8.4692	Sr_2AmUO_6	8.6044	Ba_2TbRuO_6	8.3412
Ca_2PmUO_6	8.3950	Ba_2AlMoO_6	7.9431	Ba_2TbWO_6	8.51144
Ca_2GdUO_6	8.3890	Ba_2AlWO_6	8.0341	Ba_2HoWO_6	8.4857
Ca_2TbUO_6	8.3803	Ba_2AlReO_6	7.8691	Ba_2TmVO_6	8.2003
Ca_2DyUO_6	8.3573	Ba_2AlOsO_6	7.9099	Ba_2TmWO_6	8.4439
Ca_2HoUO_6	8.3545	Ba_2AlUO_6	8.2124	Ba_2TmUO_6	8.6222
Ca_2ErUO_6	8.3436	Ba_2ScVO_6	8.0040	Ba_2YbVO_6	8.1570
Ca_2TmUO_6	8.3128	Ba_2ScWO_6	8.2476	Ba_2YbWO_6	8.4006
Ca_2YbUO_6	8.2694	Ba_2VRuO_6	7.9352	Ba_2BiUO_6	8.8539
Ca_2LuUO_6	8.2666	Ba_2VWO_6	8.1055	Ba_2AmNbO_6	8.5534
Ca_2AmUO_6	8.4695	Ba_2VUO_6	8.2837	Ba_2AmMoO_6	8.5096
Sr_2AlMoO_6	7.7686	Ba_2CrUO_6	8.2579	Ba_2AmSbO_6	8.5015
Sr_2AlWO_6	7.8596	Ba_2FeVO_6	7.9140	Ba_2AmWO_6	8.6006
Sr_2AlOsO_6	7.7354	Ba_2FeWO_6	8.1576	Ba_2AmOsO_6	8.4765
Sr_2AlUO_6	8.0379	Ba_2GaReO_6	8.0467	Ba_2AmUO_6	8.7789
Sr_2ScUO_6	8.2513	Ba_2GaOsO_6	8.0875	Pb_2ScOsO_6	8.2317
Sr_2VWO_6	7.9310	Ba_2GaUO_6	8.3900	Pb_2ScUO_6	8.5342
Sr_2VUO_6	8.1092	Ba_2YWO_6	8.4894	Pb_2RhNbO_6	8.3336
Sr_2MnWO_6	8.0465	Ba_2RhVO_6	8.0290	Pb_2RhMoO_6	8.2898
Sr_2MnOsO_6	7.9223	Ba_2RhMoO_6	8.1815	Pb_2RhSbO_6	8.2818
Sr_2FeWO_6	7.9831	Ba_2RhWO_6	8.2725	Pb_2RhBiO_6	8.4624
Sr_2GaWO_6	8.0372	Ba_2RhOsO_6	8.1483	Pb_2DyUO_6	8.7750
Sr_2GaUO_6	8.2155	Ba_2InWO_6	8.3499	Pb_2HoUO_6	8.7722
Sr_2YUO_6	8.4932	Ba_2LaWO_6	8.5879	Pb_2ErUO_6	8.7613
Sr_2RhMoO_6	8.0070	Ba_2PrUO_6	8.7786	Pb_2TmUO_6	8.7305
Sr_2RhRuO_6	7.9278	Ba_2PmMoO_6	8.4351	Pb_2LuUO_6	8.6844
Sr_2RhWO_6	8.0980	Ba_2PmRuO_6	8.3559	Pb_2AmUO_6	8.8872
Sr_2RhOsO_6	7.9739	Ba_2PmSbO_6	8.4270		
Sp. gr. *Pm*(−)3*m* (algorithm Orthogonal Matching Pursuit)					
Ba_2VBiO_6	4.3161	Pb_2VIrO_6	3.9191	Pb_2RhWO_6	4.0431
Ba_2MnBiO_6	4.3068	Pb_2CrMoO_6	3.9810	Pb_2InWO_6	4.0573

Table 3. (Contd.)

Composition	a, Å	Composition	a, Å	Composition	a, Å
Ba_2FeBiO_6	4.3309	Pb_2CrRuO_6	3.9102	Pb_2InReO_6	3.9909
Ba_2GaVO_6	3.8673	Pb_2CrWO_6	3.9975	Pb_2InOsO_6	3.9843
Ba_2GaMoO_6	3.9691	Pb_2CrOsO_6	3.9245	Pb_2InIrO_6	3.9771
Ba_2GaWO_6	3.9856	Pb_2CrIrO_6	3.9173	Pb_2InBiO_6	4.3587
Pb_2AlSbO_6	3.9782	Pb_2MnMoO_6	3.9734	Pb_2LaRuO_6	4.0798
Pb_2AlBiO_6	4.2428	Pb_2MnRuO_6	3.9027	Pb_2PrRuO_6	4.0145
Pb_2VMoO_6	3.9827	Pb_2FeRuO_6	3.9268	Pb_2NdRuO_6	4.0347
Pb_2VRuO_6	3.9120	Pb_2GaMoO_6	3.9536	Pb_2BiSbO_6	4.2570
Pb_2VReO_6	3.9328	Pb_2GaIrO_6	3.8900	Pb_2BiReO_6	4.1538
Pb_2VOsO_6	3.9262	Pb_2GaBiO_6	4.2715	Pb_2BiOsO_6	4.1473

Table 4. Prediction of the parameters for the tetragonal (or hexagonal) crystal lattice of new $A_2^{II}B^{III}B'^{V}O_6$ compounds

Composition	a, Å	c, Å	Composition	a, Å	c, Å
	Sp. gr. $I4/m$ (algorithm Ridge)	Sp. gr. $I4/m$ (algorithm Random Forest)		Sp. gr. $R(-)3$ (algorithm SAND)	Sp. gr. $R(-)3$ (algorithm ARD Regression)
Sr_2GaMoO_6	5.5927	7.8916	Ba_2BiMoO_6	6.0390	14.7809
	Sp. gr. $P6_3/mmc$ (algorithm ARD Regression)	Sp. gr. $P6_3/mmc$ (algorithm ARD Regression)	Ba_2BiRuO_6	6.0401	14.7499
Ba_2VOsO_6	5.8344	17.1422	Ba_2BiWO_6	6.0430	14.7879
Ba_2VIrO_6	5.8418	17.1460	Ba_2BiReO_6	6.0410	14.7609
Ba_2CrVO_6	5.7491	18.7279	Ba_2BiOsO_6	6.0433	14.7568

pounds, the values of the crystal lattice parameters were estimated.

CALCULATION PROCEDURE

After a peer review, information was included in the selection for computer analysis concerning 216 compounds having a composition of $A_2^{II}B^{III}B'^{V}O_6$ with a monoclinic structure (space group $P2_1/n$), 179 compounds with a cubic structure (space group $Fm(-)3m$), 27 compounds with a monoclinic structure (space group $I2/m$), 20 compounds with an ideal cubic perovskite structure (space group $Pm(-)3m$), 19 compounds with an orthorhombic structure (space group $Pbnm$), 17 compounds with a tetragonal structure (space group $I4/m$), 13 compounds with a rhombohedral structure (space group $R(-)3$), 10 compounds with a hexagonal structure (space group $P6_3/mmc$), and 15 compounds with crystal structures other than those listed above, under normal conditions.

A significant difference in the size of classes (the number of examples of compounds with space groups $P2_1/n$ and $Fm(-)3m$ is an order of magnitude greater than the number of the majority of compounds with other space groups) could result in lower predictive accuracy for compounds belonging to small classes.

The initial set of parameters for predicting the space group included the following properties of chemical elements A, B, and B': pseudopotential orbital radius (according to Zunger), ionic radius (according to Shannon), distances to internal and valence electrons (according to Schubert), ionization energies for first, second, and third electrons (E5–E7), the numbers (according to Mendeleev–Pettifor) (M1–M11 and A1–A4), quantum number, electronegativity (according to Pauling), Miedema chemical potential (E8), melting and boiling points, standard

Table 5. Prediction of the parameters for the monoclinic crystal lattice (space group $P2_1/n$) of new $Ca_2^{II}B^{III}B'^{V}O_6$ compounds

Composition	a, Å[1]	b, Å[2]	c, Å[3]	β, deg[4]	Composition	a, Å[1]	b, Å[2]	c, Å[3]	β, deg[4]
Ca_2AlMoO_6	5.3719	5.4116	7.5809	89.97	Ca_2LaMoO_6	5.6370	5.8731	8.0823	90.09
Ca_2AlWO_6	5.3777	5.4271	7.5174	90.00	Ca_2LaWO_6	5.6428	5.8886	8.0188	90.03
Ca_2AlReO_6	5.3538	5.4073	7.5789	89.97	Ca_2LaReO_6	5.6190	5.8688	8.0803	90.09
Ca_2AlOsO_6	5.3502	5.3898	7.5403	90.05	Ca_2LaOsO_6	5.6154	5.8514	8.0417	90.09
Ca_2AlIrO_6	5.3466	5.3922	7.5448	89.98	Ca_2LaIrO_6	5.6118	5.8538	8.0462	90.11
Ca_2ScMoO_6	5.4702	5.6066	7.8717	89.99	Ca_2LaBiO_6	5.7366	6.0560	8.2512	90.11
Ca_2ScRuO_6	5.4455	5.5646	7.8609	90.13	Ca_2PrVO_6	5.5790	5.7735	8.2133	90.11
Ca_2ScWO_6	5.4760	5.6221	7.8082	89.94	Ca_2PrMoO_6	5.6126	5.8341	8.1946	90.10
Ca_2ScReO_6	5.4521	5.6023	7.8697	89.94	Ca_2PrWO_6	5.6184	5.8496	8.1311	90.13
Ca_2ScIrO_6	5.4449	5.5872	7.8356	89.95	Ca_2PrReO_6	5.5945	5.8298	8.1927	90.10
Ca_2ScBiO_6	5.5697	5.7895	8.0406	90.02	Ca_2PrOsO_6	5.5909	5.8124	8.1540	90.09
Ca_2VSbO_6	5.4507	5.5291	7.89310	90.03	Ca_2PrIrO_6	5.5873	5.8148	8.1586	90.09
Ca_2VReO_6	5.4077	5.5048	7.8582	90.06	Ca_2PrBiO_6	5.7121	6.0170	8.3636	90.11
Ca_2VBiO_6	5.5253	5.6919	8.0290	90.02	Ca_2NdVO_6	5.5752	5.7670	8.2429	90.09
Ca_2CrIrO_6	5.3972	5.4665	7.6980	90.04	Ca_2NdMoO_6	5.6088	5.8276	8.2242	90.19
Ca_2CrBiO_6	5.5220	5.6687	7.9030	90.02	Ca_2NdWO_6	5.6146	5.8431	8.1607	90.13
Ca_2MnOsO_6	5.4163	5.4920	7.6727	90.12	Ca_2NdReO_6	5.5907	5.8233	8.2223	90.18
Ca_2MnBiO_6	5.5375	5.6966	7.8822	90.12	Ca_2NdOsO_6	5.5871	5.8059	8.1836	90.08
Ca_2FeWO_6	5.4430	5.5292	7.6840	90.05	Ca_2NdIrO_6	5.5835	5.8083	8.1882	90.08
Ca_2GaWO_6	5.4169	5.5060	7.6418	90.05	Ca_2NdBiO_6	5.7083	6.0105	8.3932	89.87
Ca_2GaReO_6	5.3930	5.4862	7.7034	90.06	Ca_2PmVO_6	5.5681	5.7550	8.0263	90.06
Ca_2GaOsO_6	5.3894	5.4688	7.6647	90.05	Ca_2PmNbO_6	5.6184	5.8555	8.0553	90.06
Ca_2GaIrO_6	5.3858	5.4712	7.6693	90.0	Ca_2PmMoO_6	5.6017	5.8156	8.0076	90.18
Ca_2GaBiO_6	5.5106	5.6734	7.8743	90.00	Ca_2PmRuO_6	5.5770	5.7736	7.9968	90.05
Ca_2YMoO_6	5.5574	5.7506	8.0854	90.12	Ca_2PmSbO_6	5.6267	5.8356	8.0406	89.87
Ca_2YWO_6	5.5632	5.7660	8.0219	90.09	Ca_2PmTaO_6	5.6184	5.8694	8.0157	90.06
Ca_2YReO_6	5.5393	5.7462	8.0834	90.11	Ca_2PmWO_6	5.6075	5.8310	7.9441	90.12
Ca_2YOsO_6	5.5357	5.7288	8.0448	90.07	Ca_2PmReO_6	5.5837	5.8112	8.0057	90.19
Ca_2YIrO_6	5.5321	5.7312	8.0493	90.13	Ca_2PmOsO_6	5.5800	5.7938	7.9670	90.05
Ca_2YBiO_6	5.6569	5.9334	8.2543	89.78	Ca_2PmIrO_6	5.5764	5.7962	7.9716	90.05
Ca_2RhNbO_6	5.4593	5.5722	7.9340	90.06	Ca_2PmBiO_6	5.7012	5.9984	8.1766	89.87
Ca_2RhSbO_6	5.4675	5.5523	7.9194	90.03	Ca_2SmVO_6	5.5619	5.7438	8.3538	90.0
Ca_2RhTaO_6	5.4593	5.5862	7.8944	90.05	Ca_2SmMoO_6	5.5955	5.8044	8.3351	89.87
Ca_2RhBiO_6	5.5421	5.7152	8.0553	90.03	Ca_2SmWO_6	5.6013	5.8199	8.2716	89.91
Ca_2InMoO_6	5.4992	5.6577	7.9415	90.01	Ca_2SmReO_6	5.5774	5.8001	8.3332	89.86
Ca_2InRuO_6	5.4745	5.6157	7.9307	90.06	Ca_2SmOsO_6	5.5738	5.7826	8.2945	90.02
Ca_2InWO_6	5.5050	5.6732	7.8780	90.12	Ca_2SmIrO_6	5.5702	5.7850	8.2991	90.03
Ca_2InReO_6	5.4811	5.6534	7.9396	90.11	Ca_2SmBiO_6	5.6950	5.9872	8.5040	90.0

Table 5. (Contd.)

Composition	a, Å[1]	b, Å[2]	c, Å[3]	β, deg[4]	Composition	a, Å[1]	b, Å[2]	c, Å[3]	β, deg[4]
Ca_2IrMoO_6	5.4739	5.6383	7.9055	90.07	Ca_2EuVO_6	5.5581	5.7336	8.1583	90.02
Ca_2BiMoO_6	5.5987	5.8405	8.1105	89.97	Ca_2EuMoO_6	5.5917	5.7942	8.1396	90.17
Ca_2EuWO_6	5.5975	5.8097	8.0761	90.12	Ca_2ErReO_6	5.5388	5.7369	8.0587	90.15
Ca_2EuReO_6	5.5736	5.7899	8.1376	90.17	Ca_2ErOsO_6	5.5352	5.7195	8.0201	90.20
Ca_2EuOsO_6	5.5700	5.7724	8.0990	89.97	Ca_2ErIrO_6	5.5316	5.7219	8.0246	90.20
Ca_2EuIrO_6	5.5664	5.7748	8.1035	90.01	Ca_2ErBiO_6	5.6564	5.9241	8.2296	89.72
Ca_2EuBiO_6	5.6912	5.9770	8.3085	89.91	Ca_2TmVO_6	5.5179	5.6714	8.0797	90.0
Ca_2GdMoO_6	5.5824	5.7859	8.1187	90.17	Ca_2TmMoO_6	5.5515	5.7320	8.0610	90.15
Ca_2GdWO_6	5.5882	5.8013	8.0552	90.21	Ca_2TmWO_6	5.5573	5.7475	7.9974	90.09
Ca_2GdReO_6	5.5643	5.7815	8.1168	90.17	Ca_2TmReO_6	5.5334	5.7276	8.0590	90.15
Ca_2GdOsO_6	5.5607	5.7641	8.0781	89.97	Ca_2TmOsO_6	5.5298	5.7102	8.0204	90.10
Ca_2GdIrO_6	5.5571	5.7665	8.0827	90.08	Ca_2TmIrO_6	5.5262	5.7126	8.0249	90.23
Ca_2GdBiO_6	5.6819	5.9687	8.2877	89.91	Ca_2TmBiO_6	5.6510	5.9148	8.2299	89.82
Ca_2TbVO_6	5.5410	5.7113	8.1307	90.11	Ca_2YbVO_6	5.5136	5.6602	8.0789	90.12
Ca_2TbMoO_6	5.5745	5.7719	8.1120	90.14	Ca_2YbMoO_6	5.5471	5.7208	8.0601	90.18
Ca_2TbSbO_6	5.5995	5.7919	8.1449	89.75	Ca_2YbWO_6	5.5529	5.7363	7.9966	90.12
Ca_2TbWO_6	5.5803	5.7874	8.0484	90.17	Ca_2YbReO_6	5.5291	5.7165	8.0582	90.18
Ca_2TbReO_6	5.5565	5.7676	8.1100	90.14	Ca_2YbOsO_6	5.5255	5.6991	8.0196	90.10
Ca_2TbOsO_6	5.5529	5.7501	8.0714	90.05	Ca_2YbIrO_6	5.5219	5.7015	8.0241	90.19
Ca_2TbIrO_6	5.5493	5.7525	8.0759	90.10	Ca_2YbBiO_6	5.6467	5.9037	8.2291	89.75
Ca_2TbBiO_6	5.6740	5.9548	8.2809	90.04	Ca_2LuVO_6	5.5054	5.6537	8.0387	90.14
Ca_2DyVO_6	5.5350	5.7011	8.1004	90.0	Ca_2LuMoO_6	5.5390	5.7143	8.0200	90.10
Ca_2DyMoO_6	5.5686	5.7617	8.0816	90.12	Ca_2LuWO_6	5.5448	5.7298	7.9565	90.09
Ca_2DyWO_6	5.5744	5.7772	8.0181	90.08	Ca_2LuReO_6	5.5209	5.7100	8.0180	90.10
Ca_2DyReO_6	5.5505	5.7574	8.0797	90.10	Ca_2LuOsO_6	5.5173	5.6926	7.9794	90.05
Ca_2DyOsO_6	5.5469	5.7399	8.0411	90.12	Ca_2LuIrO_6	5.5137	5.6950	7.9839	90.19
Ca_2DyIrO_6	5.5433	5.7423	8.0456	90.12	Ca_2LuBiO_6	5.6385	5.8972	8.1889	90.09
Ca_2DyBiO_6	5.6681	5.9445	8.2506	89.75	Ca_2AmVO_6	5.5799	5.7596	8.1853	90.03
Ca_2HoVO_6	5.5293	5.6909	8.1081	90.0	Ca_2AmNbO_6	5.6302	5.8601	8.2143	90.03
Ca_2HoMoO_6	5.5629	5.7515	8.0893	90.12	Ca_2AmMoO_6	5.6135	5.8202	8.1666	90.13
Ca_2HoWO_6	5.5687	5.7670	8.0258	90.08	Ca_2AmRuO_6	5.5889	5.7782	8.1558	90.13
Ca_2HoReO_6	5.5448	5.7472	8.0874	90.10	Ca_2AmSbO_6	5.6385	5.8402	8.1996	89.79
Ca_2HoOsO_6	5.5412	5.7297	8.0488	90.12	Ca_2AmTaO_6	5.6302	5.8741	8.1747	90.01
Ca_2HoIrO_6	5.5376	5.7321	8.0533	90.12	Ca_2AmWO_6	5.6193	5.8357	8.1031	90.06
Ca_2HoBiO_6	5.6624	5.9343	8.2583	89.75	Ca_2AmReO_6	5.5955	5.8159	8.1647	90.08
Ca_2ErVO_6	5.5233	5.6807	8.0794	90.0	Ca_2AmOsO_6	5.5919	5.7984	8.1260	90.01
Ca_2ErMoO_6	5.5569	5.7413	8.0607	90.15	Ca_2AmIrO_6	5.5883	5.8008	8.1306	90.10
Ca_2ErWO_6	5.5627	5.7567	7.9972	90.08	Ca_2AmBiO_6	5.7130	6.0030	8.3356	89.85

(1) ARD Regression algorithm, (2) Convex with Loop Reduction algorithm, (3) Ridge algorithm, (4) SAND algorithm.

Table 6. Prediction of the parameters for the monoclinic crystal lattice (space group $P2_1/n$) of new $A_2^{II}B^{III}B'^{V}O_6$ compounds (A = Sr, Ba or Pb)

Composition	a, Å[1]	b, Å[2]	c, Å[3]	β, deg[4]	Composition	a, Å[1]	b, Å[2]	c, Å[3]	β, deg[4]
Sr_2ScWO_6	5.7061	5.6869	7.9291	90.03	Sr_2SmReO_6	5.8075	5.8649	8.4541	90.22
Sr_2YWO_6	5.7933	5.8309	8.1428	90.21	Sr_2SmOsO_6	5.8039	5.8475	8.4154	90.18
Sr_2YBiO_6	5.8870	5.9982	8.3752	90.09	Sr_2EuWO_6	5.8276	5.8745	8.1970	90.20
Sr_2InBiO_6	5.8288	5.9054	8.2314	89.99	Sr_2EuReO_6	5.8037	5.8547	8.2585	90.23
Sr_2LaMoO_6	5.8671	5.9380	8.2032	90.21	Sr_2EuOsO_6	5.8001	5.8373	8.2199	90.28
Sr_2LaWO_6	5.8729	5.9535	8.1397	90.51	Sr_2GdWO_6	5.8183	5.8662	8.1761	90.20
Sr_2LaReO_6	5.8490	5.9336	8.2012	90.17	Sr_2GdOsO_6	5.7908	5.8289	8.1990	90.26
Sr_2LaOsO_6	5.8454	5.9162	8.1626	90.22	Sr_2TbMoO_6	5.8046	5.8368	8.2329	90.22
Sr_2LaIrO_6	5.8419	5.9186	8.1671	90.34	Sr_2TbRuO_6	5.7799	5.7948	8.2221	90.22
Sr_2LaBiO_6	5.9666	6.1208	8.3721	90.19	Sr_2TbWO_6	5.8104	5.8522	8.1694	90.20
Sr_2PrMoO_6	5.8427	5.8990	8.3155	90.22	Sr_2TbOsO_6	5.7829	5.8150	8.1923	90.20
Sr_2PrWO_6	5.8485	5.9145	8.252	90.07	Sr_2DyVO_6	5.7651	5.7659	8.2213	90.15
Sr_2PrReO_6	5.8246	5.8946	8.3136	90.20	Sr_2DyWO_6	5.8045	5.8420	8.1390	90.23
Sr_2PrOsO_6	5.8210	5.8772	8.2749	90.22	Sr_2DyOsO_6	5.7770	5.8048	8.1620	90.19
Sr_2PrIrO_6	5.8174	5.8796	8.2795	90.27	Sr_2HoVO_6	5.7594	5.7557	8.2290	90.15
Sr_2NdNbO_6	5.8556	5.9324	8.3928	90.19	Sr_2HoWO_6	5.7987	5.8318	8.1467	90.23
Sr_2NdMoO_6	5.8389	5.8925	8.3451	90.21	Sr_2HoOsO_6	5.7713	5.7946	8.1697	90.19
Sr_2NdWO_6	5.8447	5.9080	8.2816	90.24	Sr_2ErOsO_6	5.7653	5.7843	8.1410	90.21
Sr_2NdReO_6	5.8208	5.8881	8.3432	90.22	Sr_2TmVO_6	5.7480	5.7362	8.2006	90.15
Sr_2NdOsO_6	5.8172	5.87077	8.3045	90.22	Sr_2TmNbO_6	5.7982	5.8368	8.2295	90.15
Sr_2NdIrO_6	5.8136	5.8731	8.3091	90.29	Sr_2TmMoO_6	5.7816	5.7968	8.1819	90.21
Sr_2PmNbO_6	5.8485	5.9203	8.1762	90.19	Sr_2TmWO_6	5.7874	5.8123	8.1183	90.16
Sr_2PmMoO_6	5.8318	5.8804	8.1285	90.22	Sr_2TmOsO_6	5.7599	5.7751	8.1413	90.20
Sr_2PmRuO_6	5.8071	5.8384	8.1177	90.26	Sr_2YbVO_6	5.7437	5.7251	8.1998	90.12
Sr_2PmSbO_6	5.8567	5.9004	8.1615	90.29	Sr_2YbWO_6	5.7830	5.8012	8.1175	90.16
Sr_2PmTaO_6	5.8485	5.9343	8.1366	90.20	Sr_2YbOsO_6	5.7556	5.7639	8.1405	90.16
Sr_2PmWO_6	5.8376	5.8959	8.0650	90.23	Sr_2LuMoO_6	5.7691	5.7792	8.1409	90.20
Sr_2PmReO_6	5.8137	5.8761	8.1266	90.23	Sr_2LuWO_6	5.7748	5.7947	8.0774	90.11
Sr_2PmOsO_6	5.8101	5.8586	8.0879	90.22	Sr_2LuOsO_6	5.7474	5.7574	8.1003	90.18
Sr_2PmIrO_6	5.8065	5.8610	8.0925	90.27	Sr_2BiReO_6	5.8337	5.9318	8.2293	89.91
Sr_2PmBiO_6	5.9313	6.0632	8.2975	90.19	Sr_2AmVO_6	5.8100	5.8244	8.3062	90.19
Sr_2SmVO_6	5.7920	5.8087	8.4747	90.21	Sr_2AmNbO_6	5.8603	5.9250	8.3352	90.19
Sr_2SmMoO_6	5.8256	5.8693	8.4560	90.23	Sr_2AmMoO_6	5.8436	5.8851	8.2875	90.21
Sr_2SmRuO_6	5.8009	5.8273	8.4452	90.30	Sr_2AmRuO_6	5.8189	5.8431	8.2767	90.16
Sr_2SmWO_6	5.8314	5.8847	8.3925	90.18	Sr_2AmSbO_6	5.8686	5.9051	8.3205	90.19
Sr_2AmTaO_6	5.8603	5.9389	8.2956	90.17	Ba_2PmReO_6	5.9642	5.9863	8.2947	90.04
Sr_2AmReO_6	5.8255	5.8807	8.2856	90.15	Ba_2PmIrO_6	5.9570	5.9712	8.2606	90.02

Table 6. (Contd.)

Composition	a, Å[1]	b, Å[2]	c, Å[3]	β, deg[4]	Composition	a, Å[1]	b, Å[2]	c, Å[3]	β, deg[4]
Sr_2AmOsO_6	5.8219	5.8633	8.2469	90.16	Ba_2AmReO_6	5.9760	5.9909	8.4537	90.02
Sr_2AmIrO_6	5.8183	5.8657	8.2515	90.19	Pb_2DyIrO_6	6.0769	5.7554	7.7063	90.0
Sr_2AmBiO_6	5.9431	6.0679	8.4565	90.14	Pb_2HoIrO_6	6.0712	5.7452	7.7140	90.0
Ba_2PrReO_6	5.9751	6.0048	8.4817	90.04	Pb_2ErIrO_6	6.0652	5.7350	7.6854	90.04

(1) ARD Regression algorithm, (2) Convex with Loop Reduction algorithm, (3) Ridge algorithm, (4) SAND algorithm.

Table 7. Prediction of the parameters for the monoclinic crystal lattice (space group $I2/m$) of new $A_2^{II}B^{III}B'^{V}O_6$ compounds

Composition	a, Å[1]	b, Å[2]	c, Å[3]	β, deg[4]
Ba_2LaVO_6	6.0719	5.9619	8.0865	96.14
Ba_2PrVO_6	6.0405	5.9347	8.0366	95.96
Ba_2PmBiO_6	6.1496	6.1293	8.6383	90.16
Ba_2SmVO_6	6.0022	5.9067	7.9832	95.88
Ba_2SmBiO_6	6.1338	6.1190	8.6532	89.99
Ba_2GdBiO_6	6.1052	6.0920	8.6003	90.13
Ba_2NpBiO_6	6.1126	5.7853	8.6922	89.90
Ba_2PuBiO_6	6.1170	5.8743	8.6877	89.94
Ba_2AmVO_6	5.9485	5.6029	7.9832	95.77
Ba_2AmBiO_6	6.0801	5.8152	8.6531	89.89
Pb_2EuNbO_6	5.6388	6.0449	8.2646	90.12
Pb_2EuMoO_6	5.6166	5.8858	8.1018	93.50
Pb_2EuTaO_6	5.6446	6.0645	8.2677	90.12
Pb_2TbMoO_6	5.5839	5.8143	8.0534	93.49
Pb_2TbReO_6	5.5793	5.8839	7.9724	91.33
Pb_2DyNbO_6	5.5948	5.9673	8.2316	90.12
Pb_2DyMoO_6	5.5725	5.8082	8.0688	93.50
Pb_2DyRuO_6	5.5515	5.7632	7.9731	91.68
Pb_2DyTaO_6	5.6005	5.9868	8.2347	90.12
Pb_2DyWO_6	5.5815	5.8445	8.3123	92.94
Pb_2DyOsO_6	5.5607	5.9981	8.2088	87.64
Pb_2HoNbO_6	5.5873	5.9672	8.1806	90.11
Pb_2HoMoO_6	5.5650	5.8081	8.0178	93.49
Pb_2HoRuO_6	5.5440	5.7631	7.9221	91.66
Pb_2HoTaO_6	5.5930	5.9868	8.1837	90.11
Pb_2HoWO_6	5.5740	5.8445	8.2613	92.93
Pb_2HoOsO_6	5.5532	5.9981	8.1578	87.63
Pb_2ErNbO_6	5.5736	5.9421	8.1656	90.10
Pb_2ErMoO_6	5.5513	5.7830	8.0028	93.48
Pb_2ErRuO_6	5.5303	5.7380	7.9071	91.66
Pb_2ErTaO_6	5.5793	5.9617	8.1687	90.10
Pb_2ErWO_6	5.5603	5.8194	8.2463	92.93
Pb_2ErOsO_6	5.5395	5.9730	8.1428	87.62
Pb_2TmMoO_6	5.5376	5.7801	7.9998	93.48
Pb_2TmRuO_6	5.5166	5.7350	7.9041	91.65

Table 7. (Contd.)

Composition	a, Å[1]	b, Å[2]	c, Å[3]	β, deg[4]
Pb_2TmWO_6	5.5466	5.8165	8.2433	92.92
Pb_2TmOsO_6	5.5258	5.9700	8.1398	87.62
Pb_2YbVO_6	5.5315	5.9095	7.5742	95.81
Pb_2YbNbO_6	5.5851	6.0199	8.0972	90.01
Pb_2YbMoO_6	5.5628	5.8608	7.9344	93.40
Pb_2YbWO_6	5.5718	5.8972	8.1779	92.84
Pb_2YbReO_6	5.5583	5.9303	7.8534	91.24
Pb_2YbOsO_6	5.5510	6.0508	8.0744	87.54
Pb_2LuNbO_6	5.5566	5.9123	8.0915	90.10
Pb_2LuMoO_6	5.5344	5.7532	7.9287	93.48
Pb_2LuRuO_6	5.5134	5.7082	7.8330	91.66
Pb_2LuTaO_6	5.5624	5.9319	8.0946	90.10
Pb_2LuWO_6	5.5434	5.7896	8.1722	92.93
Pb_2LuOsO_6	5.5225	5.9432	8.0687	87.62

(1) Elastic Net algorithm, (2) Orthogonal Matching Pursuit algorithm, (3) Linear Regression algorithm, (4) ARD Regression algorithm.

Table 8. Prediction of crystal lattice parameters for new compounds of composition $A_2^{II}B^{III}B'^{V}O_6$ with space group *Pbnm*

Composition	a, Å[1]	b, Å[2]	c, Å[3]
Ca_2VRuO_6	5.4450	5.4891	7.7336
Ca_2VWO_6	5.4426	5.4942	7.6906
Ca_2VUO_6	5.9439	6.0479	8.5932
Ca_2CrVO_6	5.4291	5.3793	7.6249
Ca_2CrRuO_6	5.4040	5.3713	7.5380
Ca_2CrUO_6	5.9030	5.9301	8.3976
Ca_2MnVO_6	5.4164	5.5160	7.7218
Ca_2MnMoO_6	5.3955	5.5080	7.6164
Ca_2MnRuO_6	5.3914	5.5080	7.6348
Ca_2MnUO_6	5.8903	6.0668	8.4945
Ca_2FeVO_6	5.4461	5.5788	7.8200
Ca_2FeUO_6	5.9200	6.1296	8.5927
Ca_2GaVO_6	5.4429	5.5908	7.8498
Ca_2GaMoO_6	5.4220	5.5828	7.7444
Ca_2GaRuO_6	5.4179	5.5828	7.7629
Ca_2RhUO_6	5.9260	6.2269	8.6739
Ca_2InVO_6	5.5092	5.7359	7.9966
Ca_2BiMoO_6	5.5112	5.7493	7.8680
Ca_2BiRuO_6	5.5070	5.7493	7.8865
Ca_2BiWO_6	5.5047	5.7543	7.8435
Ca_2BiReO_6	5.5133	5.7837	7.9952
Ca_2BiUO_6	6.0059	6.3081	8.7461
Sr_2VIrO_6	5.5160	5.5495	7.7425
Sr_2RhUO_6	6.0257	6.2621	8.6739

(1) ARD Regression algorithm, (2) Orthogonal Matching Pursuit algorithm, (3) Orthogonal Matching Pursuit algorithm.

entropy (I11), enthalpy of atomization, thermal conductivity (I8), molar heat capacity (I10), etc. (see http://phases.imet-db.ru/elements for values).

There are a total of 105 values of the parameters of the elements for each compound plus the values of different algebraic functions of the initial parameters most informative for the classification, determined using the program [40].

RESULTS AND DISCUSSION

Table 1 lists the functions of the parameters of chemical elements that are most informative for the prediction of compounds with different crystal structures. When solving these problems, it was checked how much the accuracy of examination predicting increases when these informative functions are added to the sought regularities along with the properties of the elements. The best resulting sets of parameters of elements and algorithms, which were later used in machine learning, are highlighted in bold.

The programs based on learning algorithms for different variants of neural networks, of a linear machine, of the formation of logical patterns, of *k*-nearest neighbors, and of support vector machine have shown the best results in the cross-validation mode.

Further, using the ParLS system, the values of the crystal lattice parameters for the predicted compounds were estimated. Table 2 shows a list of algorithms the use of which in the examination recognition of the training sample in the LOOCV mode gave the best set of values for the parameters MAE, MSE, and R^2. The diagrams of the deviations of the predicted lattice parameters from the experimental ones are given in Figs. 1 and 2.

It should be noted that most of the best results were obtained using the programs included in the ParIS system [41] and based on the Orthogonal Matching Pursuit and Automatic Relevance Determination (ARD) Regression algorithms [42]. Tables 3–8 present a part of the predictions for $A_2BB'O_6$ compounds that are not yet obtained and an estimate for the parameters of their crystal lattice.

CONCLUSIONS

The analysis of the results shows that the majority of double perovskites with calcium and strontium have monoclinic distortion (space group $P2_1/n$). For compounds with barium, a doubling of the ideal cubic lattice is characteristic (space group $Fm(-)3m$). The prediction accuracy (in the sliding control mode) of the type of perovskite-like cell distortion is no less than 74%. The accuracy of estimation of the linear parameters of the lattice is within ±0.0120–0.8264 Å, whereas the accuracy for angles β in the case of lattice monoclinic distortion amounts to ±0.08°–0.74°.

The obtained predictions make it possible to reduce the number of combinations of elements in the experimental search for perovskite-like compounds with the desired space group, which should reduce the time and costs of the search. For specialists in quantum mechanical calculations, it becomes possible, although approximately, knowing the space group and the lattice parameters, to determine the arrangement of atoms in the crystal lattice of compounds not yet obtained, which in the future should make it possible to calculate some of their physical properties.

The information concerning the composition, space group, and lattice parameters of the predicted compounds that are not yet obtained after the publication of this paper should be entered into the prediction base and should expand the functionality of the Phase database (http://phases.imet-db.ru/). A user of this database, in addition to data concerning already studied inorganic compounds, should be able to obtain the results of our calculations too.

FUNDING

This work was performed under partial financial support from the Russian Foundation for Basic Research, projects 20-01-00609 and 18-07-00080, and according to the State Order no. 075-00328-21-00.

REFERENCES

1. Corredor, L.T., Téllez, D.A.L., Buitrago, D.M., Aguiar, J.A., and Roa-Rojas, J., Magnetic properties and structural characterization of Sr_2RuHoO_6 complex perovskite, *Phys. B*, 2010, vol. 407, no. 16, pp. 3085–3088. https://doi.org/10.1016/j. physb.2011.12.031
2. Hinatsu, Y., Doi, Y., and Wakeshima, M., Antiferromagnetic transitions of osmium-containing rare earth double perovskites Ba_2LnOsO_6 (Ln = rare earths), *J. Solid State Chem.*, 2013, vol. 206, pp. 300–307. https://doi.org/10.1016/j.jssc.2013.08.020
3. Li, M.-R., Retuerto, M., Deng, Z., Stephens, P.W., Croft, M., Huang, Q., Wu, H., Deng, X., Kotliar, G., Sanchez-Benitez, J., Hadermann, J., Walker, D., and Greenblatt, M., Giant magnetoresistance in the half-metallic double-perovskite ferrimagnet Mn_2FeReO_6, *Angew. Chem. Int. Ed.,* 2015, vol. 54, no. 41, pp. 12069–12073. https://doi.org/10.1002/anie.201506456
4. Sahnoun, O., Bouhani-Benziane, H., Sahnoun, M., and Driz, M., Magnetic and thermoelectric properties of ordered double perovskite Ba_2FeMoO_6, *J. Alloys Compd.*, 2017, vol. 714, pp. 704–708. https://doi.org/10.1016/j.jallcom.2017.04.180
5. Aguirre, M.H., Logvinovich, D., Bocher, L., Robert, R., Ebbinghaus, S.G., and Weidenkaff, A., High-temperature thermoelectric properties of Sr_2RuYO_6 and Sr_2RuErO_6 double perovskites influenced by structure and microstructure, *Acta Mater.*, 2009, vol. 57, no. 1, pp. 108–115. https://doi.org/10.1016/j.actamat.2008.09.003

6. Sri Gyan, D., Dwivedi, A., Roy, P., and Maiti, T., Synthesis and thermoelectric properties of Ba_2TiFeO_6 double perovskite with insight into the crystal structure, *Ferroelectrics*, 2018, vol. 536, no. 1, pp. 146–155. https://doi.org/10.1080/00150193.2018.1528922
7. Murugesan, G., Nithya, R., and Kalainathan, S., Colossal dielectric behaviour of $Sr_2TiMnO_{6-\delta}$ single crystals, *J. Cryst. Growth*, 2020, vol. 530, art. ID 125179. https://doi.org/10.1016/j.jcrysgro.2019.125179
8. Gorodea, I., Goanta, M., and Toma, M., Impact of A cation size of double perovskite A_2AlTaO_6 (A = Ca, Sr, Ba) on dielectric and catalytic properties, *J. Alloys Compd.*, 2015, vol. 632, nos. 1–2, pp. 805–809. https://doi.org/10.1016/j.jallcom.2015.01.310
9. Feraru, S., Samoila, P., Borhan, A.I., Ignat, M., Iordan, A.R., and Palamaru, M.N., Synthesis, characterization of double perovskite Ca_2MSbO_6 (M = Dy, Fe, Cr, Al) materials via sol–gel auto-combustion and their catalytic properties, *Mater. Charact.*, 2013, vol. 84, pp. 112–119. https://doi.org/10.1016/j.matchar.2013.07.005
10. Huang, Y.-H., Liang, G., Croft, M., Lehtimaki, M., Karppinen, M., and Goodenough, J.B., Double-perovskite anode materials Sr_2MMoO_6 (M = Co, Ni) for solid oxide fuel cells, *Chem. Mater.*, 2009, vol. 21, no. 10, pp. 2319–2326. https://doi.org/10.1021/cm8033643
11. Rath, M.K. and Lee, K.-T., Characterization of novel Ba_2LnMoO_6 (Ln = Pr and Nd) double perovskite as the anode material for hydrocarbon-fueled solid oxide fuel cells, *J. Alloys Compd.*, 2018, vol. 737, pp. 152–159. https://doi.org/10.1016/j.jallcom.2017.12.090
12. Ravi, S., Multiferroism in Pr_2FeCrO_6 perovskite, *J. Rare Earths*, 2018, vol. 36, no. 11, pp. 1175–1178. https://doi.org/10.1016/j.jre.2018.03.023
13. Gou, G., Charles, N., Shi, J., and Rondinelli, J.M., A-site ordered double perovskite $CaMnTi_2O_6$ as a multifunctional piezoelectric and ferroelectric–photovoltaic material, *Inorg. Chem.*, 2017, vol. 56, no. 19, pp. 11854–11861. https://doi.org/10.1021/acs.inorgchem.7b01854
14. Anderson, M.T., Greenwood, K.B., Taylor, G.A., and Poeppelmeier, K.R., B-cation arrangements in double perovskites, *Prog. Solid State Chem.,* 1993, vol. 22, no. 3, pp. 197–233. https://doi.org/10.1016/0079-6786(93)90004-B
15. Glazer, A.M., The classification of tilted octahedral in perovskites, *Acta Crystallogr., Sect. B*, 1972, vol. 28, no. 11, pp. 3384–3392. https://doi.org/10.1107/S0567740872007976
16. Howard, C.J. and Stokes, H.T., Group-theoretical analysis of octahedral tilting in perovskites, *Acta Crystallogr., Sect. B*, 1998, vol. 54, no. 6, pp. 782–789. https://doi.org/10.1107/S0108768198004200
17. Lufaso, M.W. and Woodward, P.M., Prediction of the crystal structures of perovskites using the software program SPuDS, *Acta Crystallogr., Sect. B*, 2001, vol. 57, no. 6, pp. 725–738. https://doi.org/10.1107/S0108768101015282
18. Lufaso, M.W., Barnes, P.W., and Woodward, P.M., Structure prediction of ordered and disordered multiple octahedral cation perovskites using SPuDS, *Acta Crystallogr., Sect. B*, 2006, vol. 62, no. 3, pp. 397–410. https://doi.org/10.1107/S010876810600262X
19. Askerka, M., Li, Z., Lempen, M., Liu, Y., Johnston, A., Saidaminov, M.I., Zajacz, Z., and Sargent, E.H., Learning-in-templates enables accelerated discovery and synthesis of new stable double-perovskites, *J. Am. Chem. Soc.*, 2019, vol. 141, no. 8, pp. 3682–3690. https://doi.org/10.1021/jacs.8b13420
20. Dimitrovska, S., Aleksovska, S., and Kuzmanovski, I., Prediction of the unit cell edge length of cubic $A_2^{2+}BB'O_6$ perovskites by multiple linear regression and artificial neural networks, *Cent. Eur. J. Chem.*, 2005, vol. 3, no. 1, pp. 198–215.
21. Li, W., Jacobs, R., and Morgan, D., Predicting the thermodynamic stability of perovskite oxides using machine learning models, *Comput. Mater. Sci.*, 2018, vol. 150, pp. 454–463. https://doi.org/10.1016/j. commatsci.2018.04.033
22. Majid, A., Khan, A., and Choi, T.-S., Predicting lattice constant of complex cubic perovskites using computational intelligence, *Comput. Mater. Sci.*, 2011, vol. 50, no. 6, pp. 1879–1888. https://doi.org/10.1016/j.commatsci.2011.01.035
23. Pilania, G., Mannodi-Kanakkithodi, A., Uberuaga, B.P., Ramprasad, R., Gubernatis, J.E., and Lookman, T., Machine learning bandgaps of double perovskites, *Sci. Rep.*, 2016, vol. 6, art. ID 19375. https://doi.org/10.1038/srep19375
24. Xie, S.R., Kotlarz, P., Hennig, R.G., and Nino, J.C., Machine learning of octahedral tilting in oxide perovskites by symbolic classification with compressed sensing, *Comput. Mater. Sci.,* 2020, vol. 180, art. ID 109690. https://doi.org/10.1016/j.commatsci.2020.109690
25. Xu, Q., Li, Z., Liu, M., and Yin, W.-J., Rationalizing perovskites data for machine learning and materials design, *J. Phys. Chem. Lett.*, 2018, vol. 9, no. 24, pp. 6948–6954. https://doi.org/10.1021/acs.jpclett.8b03232
26. Kiselyova, N.N., Pokrovskii, B.I., Komissarova, L.N., and Vashchenko, N.D., Simulation of the complicated oxides formation from initial components based on the cybernetic method of concept formation, *Zh. Neorg. Khim.*, 1977, vol. 22, no. 4, pp. 883–886.
27. Kiselyova, N.N., *Komp'yuternoe konstruirovanie neorganicheskikh soedinenii. Ispol'zovanie baz dannykh i metodov iskusstvennogo intellekta* (Computer-Assisted Design of Inorganic Compounds: Application of Databases and Artificial Intelligence Methods), Moscow: Nauka, 2005.
28. Zhuravlev, Yu.I., Ryazanov, V.V., and Sen'ko, O.V., *Raspoznavanie. Matematicheskie metody. Programmnaya sistema. Prakticheskie primeneniya* (Recognition. Mathematical Methods. Software System. Practical Applications), Moscow: FAZIS, 2006.
29. Kiselyova, N.N., Stolyarenko, A.V., Ryazanov, V.V., Sen'ko, O.V., Dokukin, A.A., and Podbel'skii, V.V., A system for computer-assisted design of inorganic compounds based on computer training, *Pattern Recognit. Image Anal.*, 2011, vol. 21, no. 1, pp. 88–94. https://doi.org/10.1134/S1054661811010081

30. Zhuravlev, Yu.I., Kiselyova, N.N., Ryazanov, V.V., Sen'ko, O.V., and Dokukin, A.A., Design of inorganic compounds with the use of precedent-based pattern recognition methods, *Pattern Recognit. Image Anal.*, 2011, vol. 21, no. 1, pp. 95–103. https://doi.org/10.1134/S1054661811010135

31. Kiselyova, N.N., Dudarev, V.A., Ryazanov, V.V., Sen'ko, O.V., and Dokukin, A.A., Predictions of chalcospinels with composition $ABCX_4$ (X–S or Se), *Inorg. Mater.: Appl. Res.,* 2021, vol. 12, no. 2, pp. 328–336, https://doi.org/10.1134/S2075113321020246

32. Wong, N.W., Kaduk, J.A., Luong, M., and Huang, Q., X-ray diffraction study and powder patterns of double-perovskites Sr_2RSbO_6 (R = Pr, Nd, Sm, Eu, Gd, Dy, Ho, Y, Er, Tm, Yb, and Lu), *Powder Diffr.*, 2014, vol. 29, no. 4, pp. 371–378. https://doi.org/10.1017/S0885715614000566

33. Lavat, A.E. and Baran, E.J., Structural and IR-spectroscopic characterization of some new Sr_2LnSbO_6 perovskites, *J. Alloys Compd.*, 2008, vol. 460, nos. 1–2, pp. 152–154. https://doi.org/10.1016/j.jallcom.2007.06.003

34. Evdokimov, A.A. and Men'shenina, N.F., Unit cell parameters of Ba_2REO_6, E = Nb, Ta, *Zh. Neorg. Khim.,* 1982, vol. 27, no. 8, pp. 2137–2139.

35. Saines, P.J., Kennedy, B.J., and Elcombe, M.M., Structural phase transitions and crystal chemistry of the series $Ba_2LnB'O_6$ (Ln = lanthanide and B' = Nb^{5+} or Sb^{5+}), *J. Solid State Chem.*, 2007, vol. 180, no. 2, pp. 401–409. https://doi.org/10.1016/j.jssc.2006.10.017

36. Henmi, K., Hinatsu, Y., and Masaki, N.M., Crystal structures and magnetic properties of ordered perovskites Ba_2LnNbO_6 (Ln = lanthanide elements), *J. Solid State Chem.*,1999, vol. 148, no. 2, pp. 353–360. https://doi.org/10.1006/jssc.1999.8460

37. Fu, W.T. and Ijdo, D.J.W., New insight into the symmetry and the structure of the double perovskites Ba_2LnNbO_6 (Ln = lanthanides and Y), *J. Solid State Chem.*, 2006, vol. 179, no. 4, pp. 1022–1028. https://doi.org/10.1016/j.jssc.2005.12.031

38. Ozherel'ev, I.S., Sen'ko, O.V., and Kiselyova, N.N., Method for searching outlier objects using parameters of learning instability, *Sist. Sredstva Inform.*, 2019, vol. 29, no. 2, pp. 122–134. https://doi.org/10.14357/08696527190211

39. Dineev, V.D. and Dudarev, V.A., Extendable system for multicriterial outlier detection, *CEUR Workshop Proc. (CEUR-WS.org), Suppl. Proc. 22nd Int. Conf. on Data Analytics and Management in Data Intensive Domains (DAMDID/RCDL 2020)*, 2020, vol. 2790, pp. 103–113. http://ceur-ws.org/Vol-2790/paper10.pdf

40. Senko, O.V., An optimal ensemble of predictors in convex correcting procedures, *Pattern Recognit. Image Anal.*, 2009, vol. 19, no. 3, pp. 465–468. https://doi.org/10.1134/S1054661809030110

41. Dudarev, V.A., Kiselyova, N.N., Stolyarenko, A.V., Dokukin, A.A., Senko, O.V., Ryazanov, V.V., Vashchenko, E.A., Vitushko, M.A., and Pereverzev-Orlov, V.S., An information system for inorganic substances physical properties prediction based on machine learning methods, *CEUR Workshop Proc. (CEUR-WS.org), Suppl. Proc. 22nd Int. Conf. on Data Analytics and Management in Data Intensive Domains (DAMDID/RCDL 2020)*, 2020, vol. 2790, pp. 89–102. http://ceur-ws.org/Vol-2790/paper09.pdf

42. Pedregosa, F., Varoquaux, G., Gramfort, A., Michel, V., Thirion, B., Grisel, O., et al., Scikit-learn: Machine learning in python, *J. Mach. Learn. Res.*, 2011, vol. 12, pp. 2825–2830.

Translated by O. Polyakov